

1 **Running title:** Spatial models for distance sampling
2 **Number of words:** ~4309
3 **Number of tables:** 0
4 **Number of figures:** 5
5 **Number of references:** 31

6 **Spatial models for distance sampling data:**
7 **recent developments and future directions**

8 **David L. Miller^{1*}, M. Louise Burt²,**
9 **Eric A. Rexstad², Len Thomas².**

- 10 *1. Department of Natural Resources Science, University of Rhode Island,*
11 *Kingston, Rhode Island 02881, USA*
12 *2. Centre for Research into Ecological and Environmental Modelling,*
13 *The Observatory, University of St. Andrews, St. Andrews KY16 9LZ, UK*

14 **Correspondence author. dave@ninepointeightone.net*

Summary

1. Our understanding of a biological population can be greatly enhanced by modelling their distribution in space and as a function of environmental covariates.
2. Density surface models consist of a spatial model of the abundance of a biological population which has been corrected for uncertain detection via distance sampling methods.
3. We offer a comparison of recent advances in the field and consider the likely directions of future research. In particular we consider spatial modelling techniques that may be advantageous to applied ecologists such as quantification of uncertainty in a two-stage model and smoothing in areas with complex boundaries.
4. The methods discussed are available in an R package developed by the authors and are largely implemented in the popular Windows package Distance (or are soon to be incorporated).
5. Density surface modelling enables applied ecologists to reliably estimate abundances and create maps of animal/plant distribution. Such models can also be used to investigate the relationships between distribution and environmental covariates.

Keywords: abundance estimation, Distance software, generalized additive models, line transect sampling, point transect sampling, population density, spatial modelling, wildlife surveys

39 Introduction

40 When surveying biological populations it is increasingly common to record
41 spatially referenced data, for example: coordinates of observations, habitat
42 type, elevation or (if at sea) bathymetry. Spatial models allow for vast data-
43 bases of spatially-referenced data (e.g. OBIS-SEAMAP, Halpin *et al.*, 2009)
44 to be harnessed, enabling investigation of interactions between environmental
45 covariates and population densities. Mapping the spatial distribution of a
46 population can be extremely useful, especially when communicating results
47 to non-experts. Recent advances in both methodology and software have
48 made spatial modelling readily available to the non-specialist (e.g., Wood,
49 2006; Rue *et al.*, 2009). Here we use the term “spatial model” to include any
50 model that includes spatially referenced covariates, not just smooths of loc-
51 ation. This article is concerned with combining spatial modelling techniques
52 with distance sampling (Buckland *et al.*, 2001, 2004).

53 Distance sampling takes plot sampling (counting all the individuals or
54 groups of objects within a strip or circle) and extends it to the case where
55 detection is not certain. Observers move along lines or stand at points and
56 record the distance from the line or point to the object of interest (y). These
57 distances are used to estimate the *detection function*, $g(y)$ (Fig. 2), by
58 modelling the decrease in detectability with increasing distance from the
59 line or point (conventional distance sampling, CDS). The detection function
60 may also include covariates (multiple covariate distance sampling, MCDS;
61 Marques *et al.*, 2007) which affect the scale of the detection function. From
62 the fitted detection function, the probability of detection can be estimated.

63 The estimated probability that an animal is detected, \hat{p}_i , can then be used
 64 to estimate abundance as

$$\hat{N} = \frac{A}{a} \sum_{i=1}^n \frac{1}{\hat{p}_i}, \quad (1)$$

65 where A is the area of the study region, a is the area covered by the survey
 66 (i.e., the sum of the areas of all of the strips/circles) and the summation
 67 takes place over the n observed individuals (Buckland *et al.*, 2001, Chapter
 68 3). In general distance sampling is more efficient than plot sampling because
 69 a much higher proportion of observations can be used in the analysis. Often
 70 up to half the observations in a plot sampling data set are discarded to
 71 ensure the assumption of certain detection is met. In contrast, distance
 72 sampling uses the observations that would have been discarded to model the
 73 detection (typically data are discarded beyond a given *truncation distance*
 74 during analysis).

75 When fitting the detection function in a distance sampling analysis, one
 76 assumes that the objects of interest are distributed according to some process
 77 (Buckland *et al.*, 2001, Section 2.1). It is usually possible to design surveys
 78 such that a homogenous process can be assumed so that (with respect to
 79 the line) objects are distributed uniformly. This can be achieved by ensuring
 80 that transects randomly located.

81 Estimators such as eqn (1) rely on the design of the study to ensure
 82 that abundance estimates over the whole study area (scaling up from the
 83 covered region) are valid. By contract this article focusses on *model-based*
 84 inference to extrapolate to a larger study area. Specifically, we consider the

85 use spatially explicit models to investigate the response of biological popu-
86 lations to biotic and abiotic covariates that vary over the study region. A
87 spatially-explicit model can explain the between transect variation (which
88 is often a large component of the variance in design-based estimates) and
89 so using a model-based approach can lead to smaller variance in estimates
90 of abundance. Model-based inference also enables the use of data from op-
91 portunistic surveys, for example, incidental data arising from “ecotourism”
92 cruises (Williams *et al.*, 2006).

93 Our aims in creating a spatial model of a biological population are usu-
94 ally two-fold: (i) estimating overall abundance and (ii) investigating the re-
95 lationship between abundance and environmental covariates. As with any
96 predictions that are outside the range of the data, one should heed the usual
97 warnings regarding extrapolation. For example, if a model contains eleva-
98 tion as a covariate, predictions at high, unsampled elevations are unlikely to
99 be reliable. Frequently, maps of abundance or density are required and any
100 spurious predictions can be visually assessed, as well as by plotting a histo-
101 gram of the predicted values. A sensible definition of the region of interest
102 avoids prediction outside the range of the data.

103 In this article we review the current landscape of spatial modelling of
104 distance sampling data, illustrating some recent developments most useful
105 to applied ecologists. The methods discussed have been available in the popular
106 Windows application Distance (Thomas *et al.*, 2010) for some time but the
107 recent advances covered here have been implemented in a new R package,
108 **dsm** (Miller *et al.*, 2013) and are soon to be incorporated into Distance.

109 Throughout this article a motivating data set is used to illustrate the

110 methods. These data are from a combination of several shipboard surveys
111 conducted on several cetacean species in the Gulf of Mexico. We investigate
112 47 observations of groups of pantropical spotted dolphins (*Stenella atten-*
113 *uata*); group size was recorded, as well as the Beaufort sea state at the time
114 of the observation. Coordinates for each observation and bathymetry data
115 were available as covariates for the analysis. A complete example analysis is
116 provided as an online appendix. The data used in the analysis are available
117 in the `dsm` package and `Distance`.

118 The rest of the article follows this structure: we first introduce the density
119 surface modelling approach of Hedley & Buckland (2004); explain how to
120 estimate abundance and uncertainty; describe recent advances and provide
121 practical advice regarding model fitting, formulation and checking. Before
122 concluding, we review alternative (but less mature) methods which take a
123 more direct approach to modelling spatial distance sampling data.

124 Density surface modelling

125 This section focuses on modelling the density/abundance estimation stage
126 of distance sampling, using the “count model” of Hedley & Buckland (2004),
127 which we refer to as *density surface modelling* (DSM). Both line and point
128 transects can be used but if lines are used then they are split into contigu-
129 ous *segments* (indexed by j), which are of length l_j . Segments should be small
130 enough such that neither density of objects or covariate values vary appre-
131 ciably within a segment (usually making the segments approximately square,
132 $2w \times 2w$, is sufficient). Count or estimated abundance is then modelled as

133 a smooth function of covariates using a generalized additive model (GAM;
 134 e.g. Wood, 2006). For each segment or point, the response is modelled as a
 135 function of environmental covariates that are measured at the segment/point
 136 level (z_{jk} with k indexing the covariates, e.g., location, sea surface temperat-
 137 ure, weather conditions). The area of each segment enters the model as (or
 138 as part of) an offset: the area of segment j is $A_j = 2wl_j$ and at point j is
 139 $A_j = w\pi^2$ (where w is the truncation distance).

140 COUNT AS RESPONSE

141 The model for the count per segment is:

$$\mathbb{E}(n_j) = \exp \left[\log_e (\hat{p}_j A_j) + \beta_0 + \sum_k f_k(z_{jk}) \right],$$

142 where the f_k s are smooth functions of the covariates and β_0 is an intercept
 143 term. Multiplying the segment area (A_j) by the probability of detection (\hat{p}_j)
 144 gives the *effective area* for segment j . If there are no covariates other than
 145 distance in the detection function then the probability of detection is constant
 146 for all objects observed in the segment (i.e., $\hat{p}_j = \hat{p}, \forall j$). The distribution of
 147 n_j can be modelled as overdispersed Poisson, negative binomial, or Tweedie
 148 distribution (see *Recent developments*, below).

149 Fig. 1 shows the raw observations of the dolphin data, along with the
 150 transect lines, overlaid on the depth data. A half-normal detection function
 151 was fitted to the distances and is shown in Fig. 2. Fig. 3 shows a DSM fitted
 152 to the dolphin data. The top panel shows predictions from a model where
 153 depth was the only covariate, the bottom panel shows predictions where a

154 (bivariate) smooth of spatial location was also included. The latter had a
 155 considerably lower GCV score (39.12 vs 48.46) so would be selected as our
 156 “best” model.

157 As well as simply calculating abundance estimates, relationships between
 158 covariates and abundance can be illustrated via plots of marginal smooths.
 159 The effect of depth on abundance for the dolphin data can be seen in Fig. 4.

160 ESTIMATED ABUNDANCE AS RESPONSE

161 An alternative to modelling counts is to use the per-segment/circle abund-
 162 ance using distance sampling estimates as the response. In this case we
 163 replace n_j by:

$$\hat{N}_j = \sum_{r=1}^{R_j} \frac{s_{jr}}{\hat{p}_j},$$

164 where R_j is the number observations in segment j and s_{jr} is the size of the
 165 r^{th} group in segment j (if the animals occur individually then $s_{jr} = 1, \forall j, r$).

166 The following model is then fitted:

$$\mathbb{E}(\hat{N}_j) = \exp \left[\log_e(A_j) + \beta_0 + \sum_k f_k(z_{jk}) \right],$$

167 where \hat{N}_j , as with n_j , is assumed to follow an overdispersed Poisson, negative
 168 binomial, or Tweedie distribution (see *Recent developments*, below). Note
 169 that the offset is now the area rather than effective area of the segment/point.

170 *DSM with covariates at the observation level*

171 The above models consider the case where the covariates are measured at
172 the segment/point level. Often covariates (z_{ij} , for individual/group i and
173 segment/point j) are collected on the level of observations; for example sex
174 or group size of the observed object or identity of the observer. In this case
175 the probability of detection is a function of the object (individual or group)
176 level covariates $\hat{p}(z_i)$. Object level covariates can be incorporated into the
177 model by adopting the following estimator of the per-segment abundance:

$$\hat{N}_j = \sum_{r=1}^{R_j} \frac{s_{jr}}{\hat{p}(z_{rj})}.$$

178 By not including an offset, but instead dividing the count (or estimated
179 abundance) by the area of the segment, we can also model density rather
180 than abundance. We concentrate on abundance here, see Hedley & Buckland
181 (2004) for further details on modelling density.

182 PREDICTION

183 Abundance can be predicted for the each cell in a grid over the region in
184 question and by summing predicted values over corresponding grid cells.
185 The areas of the prediction cells must be accounted for in the predictions.
186 Environmental covariates included in the model must be available at each
187 prediction cell at the required resolution (using prediction grid cells that are
188 smaller than the resolution of the spatially referenced data have no effect on
189 abundance/density estimates).

191 Estimating the variance of abundances calculated using a DSM is not straight-
 192 forward: uncertainty from the estimated parameters of the detection function
 193 must be incorporated into the spatial model. A second consideration is that
 194 in a line transect survey, adjacent segments are likely to be correlated; failure
 195 to account for this spatial autocorrelation will lead to artificially low variance
 196 estimates and hence misleadingly narrow confidence intervals.

197 Hedley & Buckland (2004) describe a method of calculating the variance
 198 in the abundance estimates using a parametric bootstrap, resampling from
 199 the residuals of the fitted model. The bootstrap procedure is as follows.

200 Denote the fitted values for the model to be $\hat{\boldsymbol{\eta}}$. For $b = 1, \dots, B$ (where
 201 B is the number of resamples required).

- 202 1. Resample (with replacement) the per-segment residuals, store the val-
 203 ues in \mathbf{r}_b .
- 204 2. Refit the model but with the response set to $\hat{\boldsymbol{\eta}} + \mathbf{r}_b$ (where $\hat{\boldsymbol{\eta}}$ are the
 205 fitted values from the original model).
- 206 3. Take the predicted values for the new model and store them.

207 From the predicted values stored in the last step the variance originating in
 208 the spatial part of the model can be calculated. The total variance of the
 209 abundance estimate (over the whole region of interest or sub-areas) can then
 210 be found by combining the variance estimate from the bootstrap procedure
 211 with the variance of the probability of detection from the detection function
 212 model (using the delta method which assumes that the two components of

213 the variance are independent; Seber, 1982).

214 The above procedure assumes that there is no correlation in space between
215 segments, if many animals are observed in a particular segment then we might
216 expect there to be high numbers in the adjacent segments. A moving block
217 bootstrap (MBB; Efron & Tibshirani, 1993, Section 8.6) can account for some
218 of this spatial autocorrelation in the variance estimation. The segments are
219 grouped together into overlapping blocks, (so if the block size is 5, block
220 one is segments 1, ..., 5, block two is segments 2, ..., 6, and so on). Then,
221 at step (2) above, resamples are taken of the blocks (contiguous collections
222 of segments) rather than individual segments within the transects. Using
223 blocks should account for some of the autocorrelation between the segments,
224 inflating the variances accordingly. However, because the block size dictates
225 the maximum amount of spatial autocorrelation accounted for, this may not
226 fully account for the autocorrelation. These bootstrap procedures can also be
227 modified to take into account detection function uncertainty by generating
228 new distances from the fitted detection function and then re-calculating the
229 offset by fitting a detection function to the new distances.

230 DSM uncertainty can be visualised via a plot of per-cell coefficient of
231 variation obtained by dividing the standard error for each cell by its predicted
232 abundance.

Recent developments

GAM uncertainty and variance propagation

Rather than using a bootstrap, one can use GAM theory to construct uncertainty estimates for DSM abundance estimates. This requires that we use the distribution of the parameters in the GAM to simulate model coefficients, using them to generate replicate abundance estimates (further information can found in Wood, 2006, page 245). Such an approach removes the need to refit the model many times, making variance estimation much faster.

Williams *et al.* (2011) go a step further and incorporate the uncertainty in the estimation of the detection function into the variance of the spatial model, albeit only when only segment level covariates are in the DSM. Their procedure is as follows:

1. Fit a density surface model.
2. Re-fit the model with an additional term that characterises the uncertainty in the estimation of the detection function (via the derivatives of the probability of detection, \hat{p}).
3. Variance estimates of the abundance calculated using standard GAM theory will include uncertainty from the estimation of the detection function.

A more complete mathematical explanation of this result is given in Appendix B.

We consider that propagating the uncertainty in this manner is not only more computationally efficient but also preferable to the moving block boot-

strap from a technical perspective. A moving block bootstrap does not fully account for spatial autocorrelation as when it reallocates blocks of residuals, it does so without considering the dependence between blocks. This can then lead to wide confidence intervals. The confidence intervals produced via variance propagation are narrower than their bootstrap equivalents, while maintaining good coverage (results of a small simulation study are given in Appendix C).

Fig. 5 shows a map of the coefficient of variation for the model which includes both location and depth covariates. Variance has been calculated using the variance propagation method.

EDGE EFFECTS

Recent work (Ramsay, 2002; Wang & Ranalli, 2007; Wood *et al.*, 2008; Scott-Hayward *et al.*, 2013; Miller & Wood, submitted) has highlighted the need to take care when smoothing over areas with complicated boundaries, e.g., those with rivers, peninsulae or islands. If two parts of the domain (either side of a river or inlet, say) are inappropriately linked by the model (the distance between the points is measured as a straight line, rather taking into account obstacles) then the boundary feature can be “smoothed across” leading to incorrect inference. Ensuring that a realistic spatial model has been fitted to the data is essential for valid inference. The soap film smoother of Wood *et al.* (2008) is appealing as the model jointly estimates boundary conditions for a complex study area along with the interior smooth. This can be helpful when uncertainty is estimated via a bootstrap as the model helps avoid large, unrealistic predictions which can plague other smoothers

280 (Bravington & Hedley, 2009).

281 Even if the study area does not have a complicated boundary, edge effects
282 can still be problematic. Miller *et al.* (in prep.) show that global smoothers
283 which have unpenalized plane components tend to cause the fitted surface to
284 increase unrealistically as predictions move further away from the locations
285 of survey effort. They suggest the use of Duchon splines (a generalisation of
286 thin plate regression splines) to alleviate the problem.

287 TWEEDIE DISTRIBUTION

288 The Tweedie distribution offers a flexible alternative to the quasi-Poisson
289 and negative binomial distributions as a response distribution when model-
290 ling count data (Candy, 2004). Through the parameter λ , many common
291 distributions arise; varying λ between 1 (Poisson) and 2 (gamma) leads to
292 a random variable which is a sum of M gamma variables where M is Pois-
293 son distributed (Jørgensen, 1987). The distribution does not change appre-
294 ciably when λ is changed by less than 0.1 therefore, a simple line search
295 over the possible values of λ is usually reasonable. Mark Bravington (pers.
296 comm.) suggested plotting the square root of the absolute value of the re-
297 siduals against fitted values; a “flat” plot (points forming a horizontal line)
298 give an indication of a “good” value for λ . We additionally suggest using the
299 metrics described in the next section for model selection.

300 Practical advice

301 Fig. 6 shows a flow diagram of the modelling process for creating a DSM.
302 The diagram shows which methods are compatible with each other and what
303 the options are for modelling a particular data set.

304 In our experience, it is sensible obtain a detection function that fits the
305 data as well as possible and only after a satisfactory detection function has
306 been obtained, begin spatial modelling. Model selection can be performed
307 for the detection function using AIC and model checking using goodness-
308 of-fit tests given in (Burnham *et al.*, 2004, Section 11.11). If animals occur
309 in groups rather than individually, bias can be incurred due to the higher
310 visibility of larger groups. It may then be necessary to include size as a
311 covariate in the detection function (see Buckland *et al.*, 2001, Section 4.8.2.4).

312 Smooth terms can be selected using (approximate) p -values in GAM. A
313 useful technique for covariate selection is to use an additional penalty for
314 each term in the GAM allowing smooth terms to be removed from the model
315 during fitting (illustrated in the example analysis; Wood, 2011). Smoothness
316 selection is performed by generalized cross validation (GCV) score, UnBiased
317 Risk Estimator (UBRE) or REstricted Maximum Likelihood (REML) score.
318 When model covariates are effectively functions of one another (e.g. depth
319 could be written as a function of location) GCV and UBRE can suffer from
320 concurvity issues which lead to failures in optimisation (Wood, 2006, Section
321 4.5.3). The minima in GCV/UBRE tend to have less pronounced minima
322 than REML so an optimal degree of smoothing may not be found, this can
323 lead to unstable models (slight changes in smoothness lead to vastly differ-

ent results; Wood, 2011). To avoid these issues REML is recommended for smoothness selection, when many spatially-referenced covariates are used. A significant drawback is that REML scores can only be used to compare models with the same fixed effects (i.e. linear terms; Wood, 2011). We highly recommend the use of standard GAM diagnostic plots. Wood (2006) provides further practical information on GAM model selection and fitting.

In the analysis of the dolphin data, we included a smooth of location. This not only nearly doubles the percentage deviance explained (27.3% to 52.7%), it also allows us to account for spatial autocorrelation (in a primitive way). One can see this when comparing the two plots in Fig. 3 and the plot of the depth in Fig. 1 the plot of the smooth of depth alone looks very similar to the raw plot of the depth data. A smooth of an environment-level covariate such as depth can be very useful for assessing the relationships between abundance and the covariate (as in Fig. 3). Caution should be employed when interpreting smooth relationships and abundance estimates, especially if there are gaps over the range of covariate values. Large counts may occur at a high value of depth but if no further observations occur at such a high value, then investigators should be skeptical of any relationship. A smooth of location can be useful although limiting the “wigglyness” of smooths of spatial location (by limiting their basis size) can be a useful way of restricting their influence whilst still allowing them to “mop up” the residual spatial correlation in the data (see the example analysis).

In the analysis presented we have converted from latitude and longitude to kilometres from the centre of the survey region (27.01, -88.3) because the bivariate smoother used (the thin plate spline; Wood, 2003) is isotropic the

349 wigglyness of the smoother in each direction is treated equally. Moving one
350 degree in latitude is not the same as moving one degree in longitude and so
351 using kilometres from the centre of the study region makes the covariates
352 isotropic (using SI units throughout would also remove the need for conver-
353 sion).

354 Direct modelling of the spatial point process

355 Rather than use a GAM to model the spatially explicit part of the model,
356 two recent articles (Johnson *et al.*, 2010; Niemi & Fernández, 2010) have used
357 a point process approach (Cox & Isham, 1980). In both cases the density
358 of objects described by an intensity function, which can include spatially-
359 referenced covariates.

360 Johnson *et al.* (2010) propose a point process-based model for distance
361 sampling data. They first assumed that the locations of all individuals in the
362 survey area (not just those observed) form a realisation of a Poisson process.
363 Parameters of the intensity function are then estimated via standard max-
364 imum likelihood methods for point processes (Baddeley & Turner, 2000). In
365 contrast to Hedley & Buckland (2004), all parameters are estimated jointly
366 so uncertainty from both the spatial pattern and the detection function is
367 incorporated into variance estimates for the abundance. This also ensures
368 that correlations between the detection function and underlying point process
369 are estimated correctly (and do not falsely inflate or deflate variance estim-
370 ates). The authors also addressed the issue of overdispersion unmodelled by
371 spatial covariates (i.e. counts that do not follow a Poisson mean-variance

372 relationship) using a post-hoc correction factor.

373 Niemi & Fernández (2010) also used Poisson processes but incorporate
374 them into a fully Bayesian approach. Model fitting proceeds in two stages:
375 first the detection function is fitted, then the spatial model (via MCMC)
376 assuming the detection function parameters are known, so detection func-
377 tion uncertainty is not incorporated in the spatial model (an extension that
378 incorporates uncertainty is, however, feasible).

379 Both of the above Poisson process models do not account for group size,
380 but both state that this could be included by considering a marked point
381 process (Cox & Isham, 1980, Section 5.5). Both methods offer direct mod-
382 elling of the point process, although with some drawbacks compared to the
383 methodology of Hedley & Buckland (2004). It should be noted that the loss
384 of efficiency from using DSM is not large (Buckland *et al.*, 2004, p. 313)
385 because distances contain little information about spatial variation due to
386 the width of the transects relative to their lengths and how small circles are
387 compared to the study area.

388 A final example of direct modelling of density is given in Royle *et al.*
389 (2004). The authors formulate an unconditional likelihood per-point/line,
390 which is a function of the unobserved transect abundances. These unob-
391 served abundances are treated as (Poisson or negative binomial) random
392 effects, which are then integrated out to give a per-transect likelihood which
393 is a function only of detection function parameters and parameters of the
394 random effects (linear functions of the environmental covariates). Due to
395 the multinomial nature of the per-transect likelihood proposed distance data
396 must be binned, resulting in a loss of information. Although an arbitrarily

397 large number of bins could be used as an approximation, this is potentially
398 computationally intensive.

399 Discussion

400 The use of model-based inference for determining abundance and spatial
401 distribution from distance sampling data presents new opportunities in the
402 field of population assessment. Inference from a sample of sightings to a
403 population in a study area does not depend upon a random sample design,
404 and therefore data from "platforms of opportunity" (Williams *et al.*, 2006)
405 can be used.

406 Unbiased estimates are dependent upon either (i) distribution of sampling
407 effort being random throughout the study area (for design-based inference)
408 or (ii) model correctness (for model-based inference). It is easier to have con-
409 fidence in the former than in the latter because our models are always wrong.
410 Nevertheless model-based inference will play an increasing role in population
411 assessment as the availability of spatially-referenced data increases.

412 The field is quickly evolving to allow modelling of more complex data
413 building on the basic ideas of density surface modelling. We expect to see
414 large advances in two areas: temporal inferences and the handling of spa-
415 tial correlation. These should become more mainstream as modern spatio-
416 temporal modelling techniques are adopted. Petersen *et al.* (2011) provided
417 a very basic framework for temporal modelling; their model included smooth
418 terms both before and after the construction of an offshore windfarm. Spa-
419 tial autocorrelation can be accounted for via approaches that explicitly intro-

420 duce correlations such as generalized estimating equations (GEEs; Hardin &
421 Hilbe, 2003) or via mechanisms such as that of Skaug (2006), which allowed
422 observations to cluster according to one of several states (e.g. “feeding” or
423 “transit”) taking into account short-term agglomerations (“hot spots”). These
424 advances should assist both modellers and wildlife managers to make optimal
425 conservation decisions.

426 Recent advances in Bayesian computation (INLA; Rue et al, 2009), make
427 a one-step, Bayesian, density surface models computationally feasible (as
428 INLA is an alternative to MCMC). We anticipate that such a direct modelling
429 technique will dominate future developments in the field.

430 Density surface modelling allows wildlife managers to make best use of
431 the available spatial data to understand patterns of abundance, and hence
432 make better conservation decisions (e.g., about reserve placement). The re-
433 cent advances mentioned here increase the reliability of the outputs from a
434 modelling exercise, and hence the efficacy of these decisions. Density surface
435 modelling from survey data is an active area of research, and we look forward
436 to further improvements and extensions in the near future.

437 Acknowledgments

438 DLM wishes to thank Mark Bravington and Sharon Hedley for their help
439 and patience in explaining and providing code for their variance propagation
440 method. Funding for the implementation of the recent advances into the
441 `dsm` package and Distance software came from the US Navy, Chief of Naval
442 Operations (Code N45), grant number N00244-10-1-0057.

443 References

- 444 Baddeley, A. & Turner, R. (2000) Practical maximum pseudolikelihood for spatial
445 point patterns. *Australian & New Zealand Journal of Statistics*, **42**, 283–322.
- 446 Bravington, M. & Hedley, S.L. (2009) Antarctic minke whale abundance estim-
447 ates from the second and third circumpolar IDCR/SOWER surveys using the
448 SPLINTR model. Paper SC/61/IA14, International Whaling Commission Sci-
449 entific Committee.
- 450 Buckland, S.T., anderson, D.R., Burnham, K.P., Laake, J.L., Borchers, D.L. &
451 Thomas, L. (2001) *Introduction to Distance Sampling*. Oxford University Press.
- 452 Buckland, S.T., anderson, D.R., Burnham, K.P., Laake, J.L., Borchers, D.L. &
453 Thomas, L. (2004) *Advanced Distance Sampling*. Oxford University Press.
- 454 Burnham, K.P., Buckland, S.T., Laake, J.L., Borchers, D.L., Marques, T.A.,
455 Bishop, J.R. & Thomas, L. (2004) Further topics in distance sampling. *Ad-
456 vanced Distance Sampling* (eds. S.T. Buckland, D.R. anderson, K.P. Burnham,
457 J.L. Laake, D.L. Borchers & L. Thomas). Oxford University Press.
- 458 Candy, S. (2004) Modelling catch and effort data using generalised linear models,
459 the Tweedie distribution, random vessel effects and random stratum-by-year
460 effects. *Ccamlr Science*, **11**, 59–80.
- 461 Cox, D.R. & Isham, V. (1980) *Point Processes*. Monographs on Applied Probability
462 and Statistics. Chapman and Hall. ISBN 9780412219108.
- 463 Efron, B. & Tibshirani, R.J. (1993) *An Introduction to the Bootstrap*. Chapman &
464 Hall/CRC. ISBN 9780412042317.
- 465 Halpin, P., Read, A., Fujioka, E., Best, B., Donnelly, B., Hazen, L., Kot, C.,
466 Urian, K., LaBrecque, E., Dimatteo, A., Cleary, J., Good, C., Crowder, L. &
467 Hyrenbach, K.D. (2009) OBIS-SEAMAP: The World Data Center for Marine
468 Mammal, Sea Bird, and Sea Turtle Distributions. *Oceanography*, **22**, 104–115.
- 469 Hardin, J. & Hilbe, J. (2003) *Generalized Estimating Equations*. Chapman and
470 Hall/CRC, London, UK.
- 471 Hedley, S.L. & Buckland, S.T. (2004) Spatial models for line transect sampling.
472 *Journal of Agricultural, Biological, and Environmental Statistics*, **9**, 181–199.
- 473 Johnson, D.S., Laake, J.L. & Ver Hoef, J.M. (2010) A model-based approach for
474 making ecological inference from distance sampling data. *Biometrics*, **66**, 310–
475 318.

- 476 Jørgensen, B. (1987) Exponential dispersion models. *Journal of the Royal Statist-*
477 *ical Society. Series B, Statistical Methodology*, **49**, 127–162.
- 478 Marques, T.A., Thomas, L., Fancy, S. & Buckland, S.T. (2007) Improving estimates
479 of bird density using multiple-covariate distance sampling. *The Auk*, **124**, 1229–
480 1243.
- 481 Miller, D.L., Rexstad, E., Burt, L., Bravington, M.V. & Hedley., S. (2013) *dsm:*
482 *Density surface modelling of distance sampling data*. R package version 2.0.1.
483 URL <http://cran.r-project.org/package=Distance>
- 484 Miller, D.L., Jones, E. & Matthiopoulos, J. (in prep.) Reliable spatial smoothing
485 without edge effects. pp. 1–8.
- 486 Miller, D.L. & Wood, S.N. (submitted) Finite area smoothing with generalized
487 distance splines. pp. 1–27.
- 488 Niemi, A. & Fernández, C. (2010) Bayesian Spatial Point Process Modeling of Line
489 Transect Data. *Journal of Agricultural, Biological, and Environmental Statistics*,
490 **15**, 327–345.
- 491 Petersen, I.K., MacKenzie, M.L., Rexstad, E.A., Wisz, M.S. & Fox, A.D. (2011)
492 Comparing pre- and post-construction distributions of long-tailed ducks *Clangula*
493 *hyemalis* in and around the Nysted offshore wind farm, Denmark: a quasi-
494 designed experiment accounting for imperfect detection, local surface features
495 and autocorrelation. CREEM technical report, University of St Andrews.
- 496 Ramsay, T. (2002) Spline smoothing over difficult regions. *Journal of the Royal*
497 *Statistical Society. Series B, Statistical Methodology*, **64**, 307–319.
- 498 Royle, J., Dawson, D. & Bates, S. (2004) Modeling abundance effects in distance
499 sampling. *Ecology*, **85**, 1591–1597.
- 500 Rue, H., Martino, S. & Chopin, N. (2009) Approximate Bayesian inference for
501 latent Gaussian models by using integrated nested Laplace approximations. *J.*
502 *R. Statist. Soc. B*, **71**, 319–392.
- 503 Scott-Hayward, L.A.S., MacKenzie, M.L., Donovan, C.R., Walker, C.G. & Ashe, E.
504 (2013) Complex Region Spatial Smoother (CReSS). *Journal of Computational*
505 *and Graphical Statistics*.
- 506 Seber, G.A.F. (1982) *The Estimation of Animal Abundance and Related Paramet-*
507 *ers*. ISBN 9781930665552.
- 508 Skaug, H.J. (2006) Markov modulated Poisson processes for clustered line transect
509 data. *Environmental and Ecological Statistics*, **13**, 199–211.

- 510 Thomas, L., Buckland, S.T., Rexstad, E.A., Laake, J.L., Strindberg, S., Hedley,
511 S.L., Bishop, J.R., Marques, T.A. & Burnham, K.P. (2010) Distance software:
512 design and analysis of distance sampling surveys for estimating population size.
513 *Journal of Applied Ecology*, **47**, 5–14.
- 514 Wang, H. & Ranalli, M. (2007) Low-rank smoothing splines on complicated do-
515 mains. *Biometrics*, **63**, 209–217.
- 516 Williams, R., Hedley, S.L., Branch, T.A., Bravington, M.V., Zerbini, A.N. & Find-
517 lay, K.P. (2011) Chilean blue whales as a case study to illustrate methods to
518 estimate abundance and evaluate conservation status of rare species. *Conserva-
519 tion Biology*, **25**, 526–535.
- 520 Williams, R., Hedley, S.L. & Hammond, P. (2006) Modeling distribution and
521 abundance of Antarctic baleen whales using ships of opportunity. *Ecology and
522 Society*, **11**, 1.
- 523 Wood, S.N. (2003) Thin plate regression splines. *Journal of the Royal Statistical
524 Society. Series B, Statistical Methodology*, **65**, 95–114.
- 525 Wood, S.N. (2006) *Generalized Additive Models: An introduction with R*. Chapman
526 & Hall/CRC.
- 527 Wood, S.N. (2011) Fast stable restricted maximum likelihood and marginal like-
528 lihood estimation of semiparametric generalized linear models. *Journal of the
529 Royal Statistical Society. Series B, Statistical Methodology*, **73**, 3–36.
- 530 Wood, S.N., Bravington, M.V. & Hedley, S.L. (2008) Soap film smoothing. *Journal
531 of the Royal Statistical Society. Series B, Statistical Methodology*, **70**, 931–955.

Figures

Fig. 1 The survey area for the example dolphin analysis, transect centrelines and observations with size of circle corresponding to the group size overlaid onto depth data.

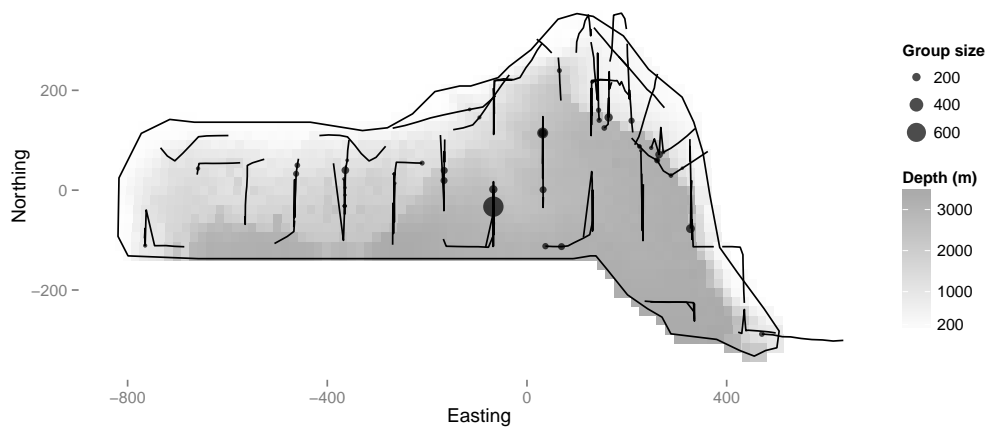


Fig. 2 Histogram of observed distances with detection function fitted to the dolphin data.

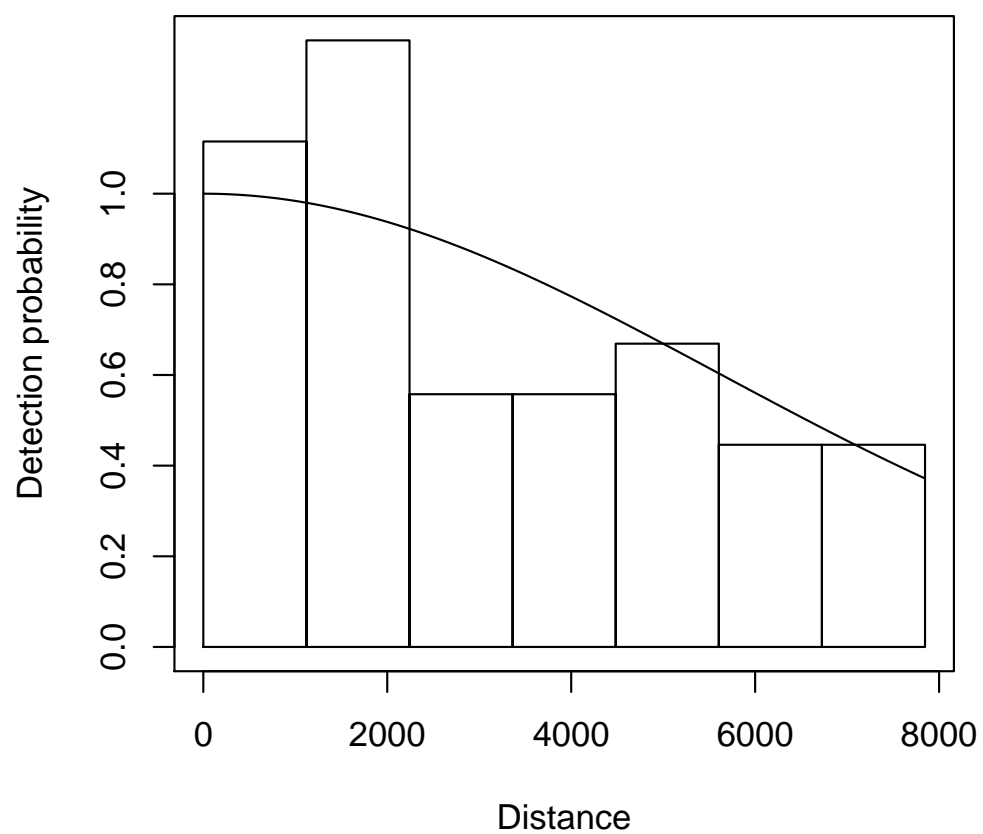


Fig. 3 Predictions for the dolphin data. Top: Predictions from the model using only depth as an explanatory variable, bottom: the model using both depth and location.

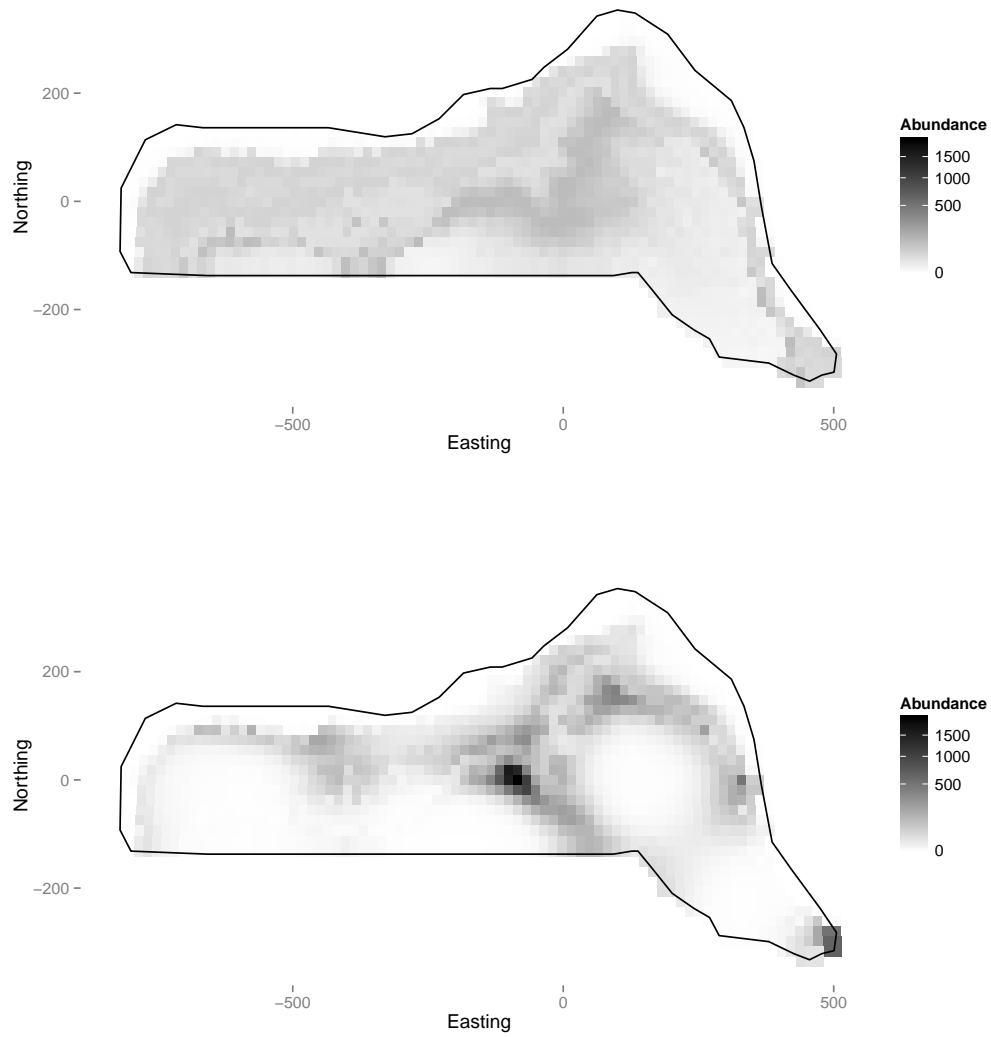


Fig. 4 Plot of the effect on the response of depth (from the model with both depth and location smooths), note that it is possible to draw a straight line between 750m and 3000m within the confidence band (between the dashed lines), so the wiggles in the smooth may not be indicative of any relationship. What is clear is that there is some effect up to about 500m. The rug ticks at the bottom of the plot indicate we have good coverage of the range of depth values in the survey area. Note that the y axis in such plots is on the scale of the link function (log in this case), so care should be taken in their interpretation.

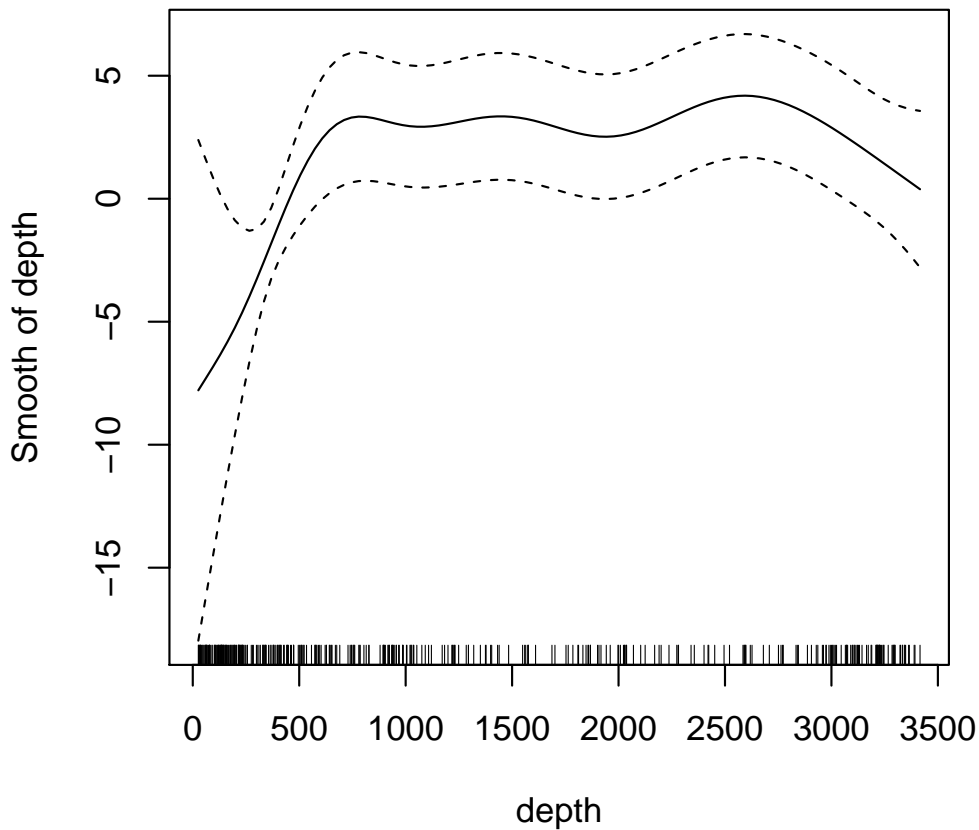


Fig. 5 Plot of coefficient of variation map for the model with smooths of both depth and location. Uncertainty was estimated using the variance propagation method of Williams *et al.* (2011). As might be expected, there is high uncertainty where there is low sampling effort (Fig. 1).

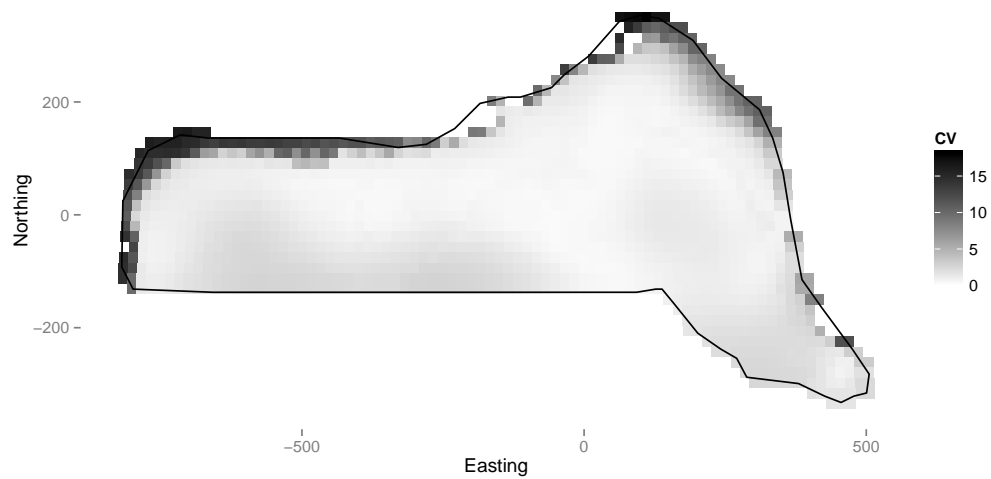


Fig. 6 Flow diagram showing the modelling process for creating a density surface model.

